Communication

Asymmetry in C–C COSY Spectra Provides Information on Ligand Geometry in Paramagnetic Proteins

Ivano Bertini, Beatriz Jimnez, Mario Piccioli, and Luisa Poggi

J. Am. Chem. Soc., **2005**, 127 (35), 12216-12217• DOI: 10.1021/ja051058m • Publication Date (Web): 12 August 2005

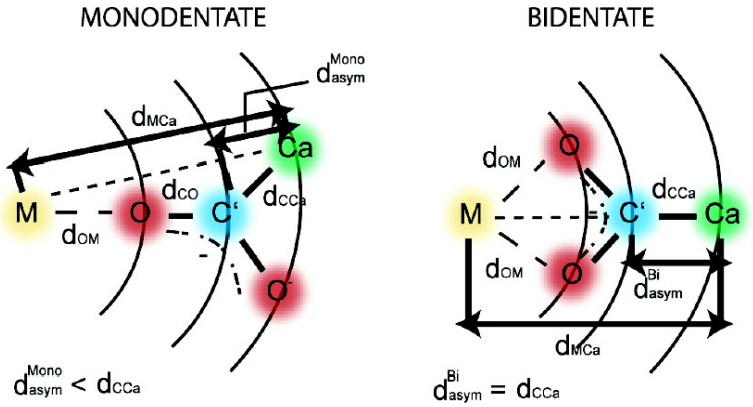

More About This Article

Additional resources and features associated with this article are available within the HTML version:

- Supporting Information
- Links to the 4 articles that cite this article, as of the time of this article download
- Access to high resolution figures
- Links to articles and content related to this article
- Copyright permission to reproduce figures and/or text from this article

View the Full Text HTML

J|A|C|S
COMMUNICATIONS

Published on Web 08/12/2005

Asymmetry in $^{13}C-^{13}C$ COSY Spectra Provides Information on Ligand Geometry in Paramagnetic Proteins

Ivano Bertini,*,† Beatriz Jiménez,† Mario Piccioli,† and Luisa Poggi‡

Magnetic Resonance Center, University of Florence, Via Luigi Sacconi 6, 50019 Sesto Fiorentino, Florence, Italy, and Department of Chemistry, Ecole Normale Supérieure, 24 Rue Lhomond, 75005 Paris, France

Received February 18, 2005; E-mail: ivanobertini@cerm.unifi.it

A major problem in the solution structure determination of metalloproteins by NMR spectroscopy is the characterization of the metal binding site.[1] Recently, a protocol based on a combination of ^{13}C direct detection and of paramagnetic versions of classic double- and triple-resonance experiments has permitted the full assignment of the C═O groups coordinating the paramagnetic ion in the cerium-substituted calcium binding protein, calbindin D_{9k} (CaCeCb hereafter).[2]

In an effort to further characterize the coordination sphere of the paramagnetic ion, we have employed a simplified approach based on the asymmetry of a $^{13}C-^{13}C$ COSY spectrum. COSY is an intrinsically symmetric experiment.[3,4] However, the symmetry is broken when the recycle delay is short enough to prevent complete recovery to equilibrium of the bulk magnetization.[5] Additionally, when the J couplings are of the same order of magnitude, if not smaller, than transverse relaxation rates, the efficiency of coherence transfer from spin I to S, and vice versa can be differentially affected by transverse relaxation, thus further contributing to remove the symmetry in COSY experiments. We will show here how an appropriate choice of acquisition times t_{1max}, t_{2max}, and recycle delay gives rise to COSY spectra in which the information collected on both sides of the spectrum is directly related to the orientation of the internuclear vectors ($C^{\alpha}-C'$) with respect to the metal ion.

In paramagnetic proteins, scalar couplings near the paramagnetic ion are quenched by hyperfine relaxation, which depends on γ^2 of the investigated nucleus. This is why $^{13}C-^{13}C$ COSY is more efficient than the corresponding ^1H experiment to identify resonances in the proximity of a paramagnetic center.[2,6−10]A phase-insensitive COSY experiment should be displayed in magnitude mode, where the data point matrix is Fourier transformed with a sine bell procedure applied in both dimensions.[11] For $C^{\alpha}-C'$ connectivities (or for side-chain $C^{OO}-C^{ali}$ scalar couplings, for which the same considerations hold), the ratio between cross-peak intensity on the upper diagonal (I_{up} hereafter) and on the lower diagonal (I_{lo}) of a $^{13}C-^{13}C$ COSY spectrum is given by (see Supporting Information for details):

$$\frac{I_{up}}{I_{lo}} = \underbrace{\frac{M^{C\alpha}}{M^{C'}}}_{A} \underbrace{\frac{(t_{1max}^2 + T_{2C'}^2) \times (t_{2max}^2 + T_{2C\alpha}^2)}{(t_{1max}^2 + T_{2C\alpha}^2) \times (t_{2max}^2 + T_{2C'}^2)}}_{B} \qquad (1)$$

where $M^{C\alpha}$ and $M^{C'}$ are the initial bulk magnetizations of C^{α} and C' at steady-state conditions; T_2 is the characteristic time for the decay of the transverse magnetization, and t_{1max} and t_{2max} are the acquisition times in the indirect and in the direct dimension, respectively. The $^{13}C-^{13}C$ COSY experiment presented in this work was recorded with a t_{1max} of 5.7 ms and a t_{2max} of 19.4 ms, and its upper and lower off diagonal regions are shown in Figure 1. Peak intensities in the upper off diagonal part are, on average, a factor of 3 larger than those of the lower off diagonal region (for example, peaks 1 and 2). However, there are peaks with a ratio larger than the general trend (e.g., peaks 3 and 4), others that are almost symmetrical (peaks 5−7), and even some which are barely observed in panel A but are clearly detected in panel B (peaks 8 and 9). Under the aforementioned experimental conditions and for diamagnetic signals (for which $T_2^{C'}$, $T_2^{C\alpha}$ values of hundreds of milliseconds are expected), $T_2^{C'}$, $T_2^{C\alpha} \gg t_{1max}$, t_{2max}, and term B equals 1. For paramagnetic signals, $T_2^{C'}$ and $T_2^{C\alpha}$ values are comparable to the chosen acquisition times, and term B is no longer equal to 1. For any given value of $T_2^{C'}$, the ratio B is 1 when $T_2^{C\alpha} = T_2^{C'}$, while it is smaller than 1 for $T_2^{C\alpha} > T_2^{C'}$. For term A, if paramagnetic contributions to relaxation occur, the bulk magnetization at steady-state conditions is equal to the equilibrium bulk magnetization ($M^C \approx M^{C}_0$), and so A equals 1, while for signals far enough from the metal center the ratio $M^{C\alpha}/M^{C'}$ is given by the ratio of the diamagnetic relaxation rates $R_{1D}{}^{C\alpha}/R_{1D}{}^{C'}$ (see Supporting Information for details).

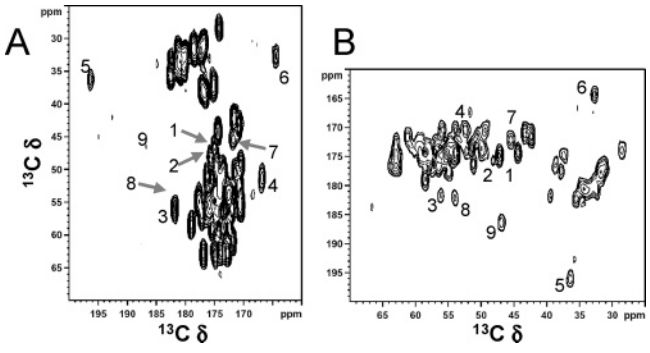

Figure 1. Upper off diagonal (A) and lower off diagonal (B) parts of $^{13}C-^{13}C$ COSY spectrum of CaCeCb showing the $C^{\alpha}-C'$ correlations, recorded at 300 K on a Bruker Avance 700 (16.4 T), incorporating a triple-resonance probe customized for ^{13}C direct detection. ^{13}C, ^{15}N, and ^1H carriers were set at 150, 120, and 3.5 ppm, respectively. The spectrum was acquired using a 300 ppm spectral window in both dimensions. A 2048 × 300 data point matrix was acquired using 512 scans each fid, 19.4 ms, and 300 ms as acquisition and recycle delays, respectively. The value of t_{1max} was 5.7 ms. ^1H and ^{15}N were decoupled during the entire sequence. The spectrum was recorded in magnitude mode,[9] and due to the available resolution, no J_{CC} coupling is visible. Peaks 8 and 9 in panel A are below the threshold.

Equation 1 does not take into account $C^{\alpha}-C^{\beta}$ couplings and, therefore, can be quantitatively exploited only if a complementary experiment is recorded on a diamagnetic analogue, provided here by the lanthanum monosubstituted calbindin (CaLaCb).[2,12] The ratio between peak intensities observed in CaCeCb and those observed in CaLaCb will be such as (see Supporting Information for details):

$$\left(\frac{^{Ce}I_{up}}{^{Ce}I_{lo}} \times \frac{^{La}I_{lo}}{^{La}I_{up}}\right) = C \times B^{Ce} \qquad (2)$$

† University of Florence.
‡ Ecole Normale Supérieure.

10.1021/ja051058m CCC: $30.25

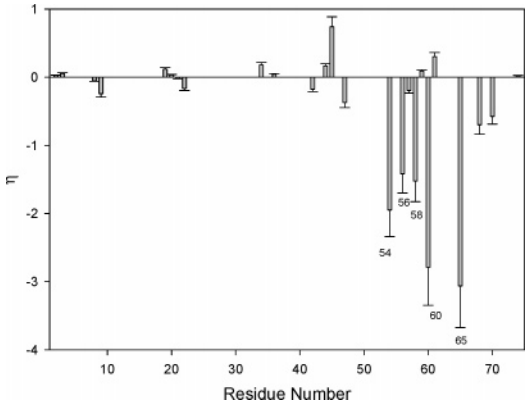

Figure 2. Logarithmic ratio between peak intensities observed in the CaCeCb derivative and those observed in the corresponding diamagnetic CaLaCb derivative. Error bars are estimated applying error propagation.

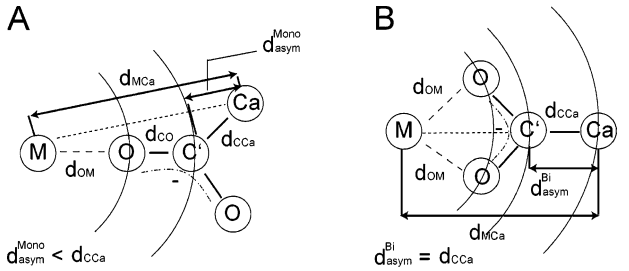

Figure 3. Schematic representation of the coordination geometry of a monodentate (A) and bidentate (B) carboxylate ligand. "Ca" denotes aliphatic carbons, while "C′" represents carboxylic carbons.

where the first term, C, is purely R_1 dependent, and the second is R_2 dependent. The first term (C) is such that $\lim_{R1P\to 0} C = 1$ and $\lim_{R1P\to\infty} C = R_{1D}{}^{C'}/R_{1D}{}^{C\alpha}$.

Equation 2 can be rewritten in the logarithmic form:

$$\ln\left(\frac{{}^{Ce}I_{up}}{{}^{Ce}I_{lo}} \times \frac{{}^{La}I_{lo}}{{}^{La}I_{up}}\right) = \ln C + \ln B^{Ce} = \eta \qquad (3)$$

The η value is expected to be zero far from the paramagnetic center and to be dominated by the R_2 dependent part in the first coordination sphere, where C is close to the limit value $R_{1D}{}^{C'}/R_{1D}{}^{C\alpha}$ so that $\ln C \leq 0$ because, for this system, at this magnetic field, $R_{1D}{}^{C'} < R_{1D}{}^{C\alpha}$.[14] Since R_{2P} is proportional to $d_{MC}{}^{-6}$, where d_{MC} is the metal−carbon distance, a C═O ligand will have $\Delta R_{2P} < 0$ (i.e., $d_{MC'} < d_{MC\alpha}$), where $\Delta R_{2P} = R_{2P}{}^{C\alpha} - R_{2P}{}^{C'}$. Therefore, one should expect $\eta < 0$ for all the metal-binding groups.

Results are shown in Figure 2. As expected, all the observed values of η are zero, within the experimental error, with the exception of a small number of signals that present high negative values. They correspond to Asp54 C^{γ} (peak 5 in Figure 1), Asn56 C^{γ} (peak 6), Asp58 C^{γ} (peak 7), Glu60 C′ (peak 8), and Glu65 C^{δ} (peak 9). These are the signals corresponding to the quaternary carbons directly bound to the metal ion via a C═O−Ce coordination.[2] Therefore, this method allows one to identify resonances belonging to metal-bound groups independently of the availability of a sequence-specific assignment. Furthermore, the coordination geometry of side-chain residues can be identified from the different η values observed for the four side-chain C═O's coordinating the metal ion. The bidentate coordination geometry leads to a larger, in absolute value, ΔR_{2P} value (and therefore to a more negative η value) than those found for monodentate ligands, as pictured in Figure 3. For both C^{ali} and C^{OO-}, R_{2P} is proportional to d^{-6}, d being the C−Ce distance. The ΔR_{2P} value can, therefore, be related to $d_{asym}{}^{-6}$, being $d_{asym} = d_{MC\alpha} - d_{MC'}$. Indeed, as shown in Figure 3, for a monodentate ligand, $d_{asym}^{mono} < d_{C'C\alpha}$, while for a bidentate side-chain, $d_{asym}^{bi} = d_{C'C\alpha}$. We can, therefore, conclude that $d_{asym}^{bi} > d_{asym}^{mono}$, which means that $|\Delta R_{2P}^{bi}| > |\Delta R_{2P}^{mono}|$. On these bases and according to Figure 2 values, Glu65 is bidentate. This is consistent with the published crystallographic data available on the PDB databank[13] (PDB entry 4ICB), where Glu65 C^{δ} is found to coordinate the metal ion in a bidentate fashion, while Asp54 C^{γ}, Asn56 C^{γ}, and Asp58 C^{γ} are purely monodentate.

The backbone CO of Glu60, which can only bind the metal in a monodentate fashion, shows a η value larger than expected. Independent measurements have shown that R_2 of the Glu60 C′ is remarkably larger than the sum of the predicted paramagnetic and diamagnetic contributions to the transversal relaxation rate. Relaxation interference between Curie spin (CS) relaxation and chemical shift anisotropy (CSA) of backbone carbonyls coordinating a paramagnetic metal may account for this behavior. Due to its angular dependence, this effect is expected to be much smaller, if any, for side-chain than for backbone C═O's.

The asymmetry of a paramagnetic $^{13}C-{}^{13}C$ COSY acquired with a specific combination of acquisition times and recycle delay allows one to easily identify the coordinating residues of a paramagnetic metal ion with a straightforward single-experiment approach. To our knowledge, this is also the only NMR method available to distinguish between monodentate and bidentate coordinating side-chain carbonyls.

Acknowledgment. B.J. is an EMBO Long Term Fellow. L.P. acknowledges MENESR-MDR France for a fellowship. This work was supported by COFIN-2003 (Nov 03-Nov 05) Italy, and by the European Union, RTD Program (HPRI-CT-2001-50026).

Supporting Information Available: Analytical derivation and three-dimensional plots of eqs 1−3 and cross-sections of COSY spectrum. This material is available free of charge via the Internet at http://pubs.acs.org.

References

(1) Bertini, I.; Luchinat, C.; Piccioli, M. *Methods Enzymol.* **2001**, *339*, 314−340.

(2) Bertini, I.; Lee, Y. M.; Luchinat, C.; Piccioli, M.; Poggi, L. *ChemBioChem* **2001**, *2*, 550−558.

(3) Griesinger, C.; Gemperle, C.; Sorensen, O. W.; Ernst, R. R. *Mol. Phys.* **1987**, *62*, 295−332.

(4) Sorensen, O. W.; Griesinger, C.; Ernst, R. R. *Chem. Phys. Lett.* **1987**, *135*, 313−318.

(5) Bertini, I.; Luchinat, C.; Piccioli, M.; Tarchi, D. *Concepts Magn. Reson.* **1994**, *6*, 307−335.

(6) Kolczak, U.; Salgado, J.; Siegal, G.; Saraste, M.; Canters, G. W. *Biospectroscopy* **1999**, *5*, S19−S32.

(7) Arnesano, F.; Banci, L.; Bertini, I.; Felli, I. C.; Luchinat, C.; Thompsett, A. R. *J. Am. Chem.* Soc. **2003**, *125*, 7200−7208.

(8) Machonkin, T. E.; Westler, W. M.; Markley, J. L. *J. Am. Chem. Soc.* **2002**, *124*, 3204−3205.

(9) Machonkin, T. E.; Westler, W. M.; Markley, J. L. *J. Am. Chem. Soc.* **2004**, *126*, 5413−5426.

(10) Kostic, M.; Pochapsky, S. S.; Pochapsky, T. C. *J. Am. Chem. Soc.* **2002**, *124*, 9054−9055.

(11) De Marco, A.; Wüthrich, K. *J. Magn. Reson.* **1976**, *24*, 201−204.

(12) Bertini, I.; Donaire, A.; Jimenez, B.; Luchinat, C.; Parigi, G.; Piccioli, M.; Poggi, L. *J. Biomol. NMR* **2001**, *21*, 85−98.

(13) Berman, H. M.; Westbrook, J.; Feng, Z.; Gilliland, G.; Bhat, T. N.; Weissig, H.; Shindyalov, I. N.; Bourne, P. E. *Nucleic Acids Res.* **2000**, *28*, 235−242.

(14) Fischer, M. W.; Zeng, L.; Pang Y.; Zuiderweg, E. R. P. *J. Am. Chem. Soc.* **1997**, *119*, 12629−12642.

JA051058M